Targeting Pyruvate Carboxylase Reduces Gluconeogenesis and Adiposity and Improves Insulin Resistance

Naoki Kumashiro,[1,2] Sara A. Beddow,[3] Daniel F. Vatner,[2] Sachin K. Majumdar,[2] Jennifer L. Cantley,[1,2] Fitsum Guebre-Egziabher,[2] Ioana Fat,[2] Blas Guigni,[2] Michael J. Jurczak,[2] Andreas L. Birkenfeld,[2] Mario Kahn,[2] Bryce K. Perler,[2] Michelle A. Puchowicz,[4] Vara Prasad Manchem,[5] Sanjay Bhanot,[5] Christopher D. Still,[6] Glenn S. Gerhard,[6] Kitt Falk Petersen,[2] Gary W. Cline,[2] Gerald I. Shulman,[1,2,7] and Varman T. Samuel[2,3]

We measured the mRNA and protein expression of the key gluconeogenic enzymes in human liver biopsy specimens and found that only hepatic pyruvate carboxylase protein levels related strongly with glycemia. We assessed the role of pyruvate carboxylase in regulating glucose and lipid metabolism in rats through a loss-of-function approach using a specific antisense oligonucleotide (ASO) to decrease expression predominantly in liver and adipose tissue. Pyruvate carboxylase ASO reduced plasma glucose concentrations and the rate of endogenous glucose production in vivo. Interestingly, pyruvate carboxylase ASO also reduced adiposity, plasma lipid concentrations, and hepatic steatosis in high fat–fed rats and improved hepatic insulin sensitivity. Pyruvate carboxylase ASO had similar effects in Zucker Diabetic Fatty rats. Pyruvate carboxylase ASO did not alter de novo fatty acid synthesis, lipolysis, or hepatocyte fatty acid oxidation. In contrast, the lipid phenotype was attributed to a decrease in hepatic and adipose glycerol synthesis, which is important for fatty acid esterification when dietary fat is in excess. Tissue-specific inhibition of pyruvate carboxylase is a potential therapeutic approach for nonalcoholic fatty liver disease, hepatic insulin resistance, and type 2 diabetes. ***Diabetes*** **62:2183–2194, 2013**

A key step in the pathogenesis of type 2 diabetes is the development of increased hepatic gluconeogenesis and fasting hyperglycemia (1–3). Hepatic gluconeogenesis is enzymatically regulated primarily by four gluconeogenic enzymes: phosphoenolpyruvate carboxykinase (PEPCK), fructose-1,6-bisphosphatase (FBP1), glucose-6-phosphatase (G6PC), and pyruvate carboxylase (4–7). Increased hepatic gluconeogenesis is often ascribed to transcriptional regulation of two key gluconeogenic enzymes, PEPCK and G6PC, through an intricate web of transcriptional factors and cofactors (8–12). Yet, despite the high degree of transcription regulation for these enzymes, the control they exert over gluconeogenic flux is relatively weak (13–16). We recently reported that hepatic expression of PEPCK and G6PC mRNA was not related to fasting hyperglycemia in two rodent models of type 2 diabetes and in patients with type 2 diabetes (17). Thus, we hypothesized that other mechanisms must account for increased hepatic gluconeogenesis and fasting hyperglycemia in type 2 diabetes.

Pyruvate carboxylase catalyzes the first committed step for gluconeogenesis and is well poised to regulate hepatic glucose production. Pyruvate carboxylase is allosterically activated by acetyl-CoA (18). However, increased expression of pyruvate carboxylase has been reported in rodent models of type 1 diabetes (19,20) and in obese Zucker Diabetic Fatty (ZDF) rats (21). Here, we performed a comprehensive assessment of hepatic gluconeogenic enzyme expression and discovered a strong association between pyruvate carboxylase protein expression and glycemia in humans. We then quantified the effect of pyruvate carboxylase on glucose and lipid metabolism in vivo in multiple rodent models by using a specific antisense oligonucleotide (ASO) to decrease pyruvate carboxylase expression selectively in liver and adipose tissue. Although chemical inhibitors of pyruvate carboxylase can acutely reduce glucose production (22), these compounds lack tissue specificity. ASOs primarily decrease expression in liver and adipose, but not in other key tissues such as pancreas, muscle, or neurons (23,24). Thus, this approach permits us to chronically decrease pyruvate carboxylase expression in select tissues of adult animals, without altering expression in tissues where this enzyme supports anaplerotic flux (e.g., β-cells, astrocytes), and also avoids any potentially confounding compensatory effects that may occur in germline gene-knockout rodent studies. We assessed the effects of pyruvate carboxylase ASO in several rodent models, quantifying changes in glucose metabolism, lipid metabolism, and insulin sensitivity in vivo.

RESEARCH DESIGN AND METHODS

Animals. Male Sprague-Dawley (SD) rats (160–180 g), ZDF rats (7 weeks old), and C57/BL6 mice (7 weeks old) were received from Charles River Laboratories (Wilmington, MA) and given at least 3 days to acclimate. Rats and mice were housed on a 12:12-h light/dark cycle and received food and water ad libitum. Chow consisted of regular rodent chow (60% carbohydrate, 10% fat, 30% protein calories) and a high-fat diet (Dyets 112245: 26% carbohydrate, 59% fat, 15% protein calories; Dyets, Inc., Bethlehem, PA). ZDF rats were fed Purina Laboratory Diet 5008 (56.4% carbohydrate, 16.7% fat, 26.8% protein calories). Body weight was monitored twice weekly.

From the [1]Howard Hughes Medical Institute, Yale University School of Medicine, New Haven, Connecticut; the [2]Department of Internal Medicine, Yale University School of Medicine, New Haven, Connecticut; the [3]Veterans Affairs Medical Center, West Haven, Connecticut; the [4]Department of Nutrition, Case Western Reserve University, Cleveland, Ohio; [5]ISIS Pharmaceuticals, Carlsbad, California; the [6]Weis Center for Research, Geisinger Clinic, Danville, Pennsylvania; and the [7]Department of Cellular & Molecular Physiology, Yale University School of Medicine, New Haven, Connecticut.

Corresponding author: Varman T. Samuel, varman.samuel@yale.edu.

Received 24 September 2012 and accepted 9 February 2013.

DOI: 10.2337/db12-1311

This article contains Supplementary Data online at http://diabetes.diabetesjournals.org/lookup/suppl/doi:10.2337/db12-1311/-/DC1.

ASOs were injected intraperitoneally at a dose of 75 mg/kg weekly for at least 4 weeks. For high fat–fed (HFF) rats, the ASO injection was started on the same day as the high-fat diet. For fasting experiments, rats were fasted overnight (~14 h). Rats underwent the placement of jugular venous catheters for blood sampling and carotid artery catheters for infusion ~10 days before the terminal studies. They recovered their presurgical weights by 5–7 days after the operation. All procedures were approved by the Yale University School of Medicine Institutional Animal Care and Use Committee.

Study population. All patients who were enrolled in the Bariatric Surgery Program of the Geisinger Center for Nutrition and Weight Management between October 2004 and October 2010 were offered the opportunity to participate in this study and some other studies (25). More than 90% of patients consented to participate. Patients underwent a preoperative assessment and preparation program of monthly visits, during which time a comprehensive set of clinical and laboratory measures were obtained. Although patients lost an average of ~9% body weight during the year before surgery, their weight remained relatively stable during the preoperative period between blood sampling and liver biopsy, with an average percentage change in body weight of 0.41%. The protocol was approved by the institutional review boards of the Geisinger Clinic and Yale University, and all participants provided written informed consent.

Liver biopsies. During the bariatric surgery, a wedge biopsy sample (250–300 mg) was obtained from the right lobe of the liver 10 cm to the left of the falciform ligament and flash frozen in liquid nitrogen for subsequent analysis.

Selection of ASOs. Rats and mice pyruvate carboxylase and control ASOs were designed and produced as previously described (26). The sequence 5-GCCAGACTTCATGGTAGCCG-3 (ISIS-330749) was selected for both rats and mice pyruvate carboxylase and the sequence 5-CCTTCCCTGAAGGTTCCTCC-3 (ISIS-141923) was selected as the control ASO.

RT-PCR. RT-PCR was performed as previously described (26,27). Primer sequences are described in Supplementary Table 3.

Western blotting. For gluconeogenic enzymes, liver proteins were compartmentalized into three fractions, namely, a mitochondria-containing fraction, a cytoplasm fraction, and a microsomal fraction, as previously reported (27–29). G6PC was detected in the microsomal fraction, cytosolic PEPCK (C-PEPCK) and FBP1 were detected in the cytoplasmic fraction, and pyruvate carboxylase and mitochondrial PEPCK (M-PEPCK) were detected in the mitochondria-containing fraction. The sheep polyclonal C-PEPCK antibody was a gift from Daryl Granner (Vanderbilt University Medical Center). G6PC, pyruvate carboxylase, and M-PEPCK antibodies were purchased from Santa Cruz Biotechnology, Inc. (Santa Cruz, CA). FBP1 was purchased from Abcam, Inc. (Cambridge, MA).

For immunoprecipitation, the mitochondria fraction was extracted as above, but 50 mmol/L *N*-ethylmaleimide, 250 mmol/L nicotinamide, and 50 mmol/L sodium fluoride were added in the buffer. Mitochondria protein (1 mg) was mixed with 4 μg pyruvate carboxylase antibody and protein A/G (Santa Cruz Biotechnology, Inc.). Homogenization buffer was added up to 500 μL and incubated overnight. After overnight incubation, samples were washed three times with homogenization buffer containing 1% NP-40, and then 40 μL sample buffer was added and boiled for 5 min. Ubiquitin was detected using ubiquitin antibody (Covance, Inc., Dedham, MA) and then stripped and reprobed with pyruvate carboxylase antibody.

Whole cell lysates preparation, protein kinase C (PKC) translocation assay, and Western blotting for all the proteins were done as previously described (26,27,30).

Biochemical analysis and calculations. Plasma C-peptide was measured by radioimmunoassay kit (Millipore, Billerica, MA). Plasma lactate concentration was measured on Roche Cobas Mira Plus (Analytical Instruments, LLC, Golden Valley, MN) using the lactate reagent test kit (Pointe Scientific, Inc., Canton, MI). The others were measured as previously described (26,27).

Mixed-meal loading test. Chronically catheterized rats treated with ASOs were fasted overnight and given a mixed meal (15 kcal/kg body weight, Ensure Plus Ready-to-Drink Homemade Vanilla [Abbott Nutrition, Columbus, OH], 57% carbohydrate, 28% fat, 15% protein calories) through a gastric catheter. Blood was taken from the venous catheter at the indicated time in the results.

Pyruvate tolerance test. A pyruvate tolerance test was performed as previously described (30).

Hepatic lipid metabolites assay. Hepatic triglyceride and diacylglycerol contents were determined as previously described (26,27).

Mice body composition, metabolic parameters, and physical activity. Body composition was assessed by ^{1}H magnetic resonance spectroscopy using a Bruker Minispec analyzer mq10 (Bruker Optics, Inc., Billerica, MA). Metabolic parameters, energy expenditure, and food intake were measured using the comprehensive animal metabolic monitoring system (Columbus Instruments, Columbus, OH).

Hyperinsulinemic-euglycemic clamp studies. Hyperinsulinemic-euglycemic clamp studies were performed as previously described (26,31). Insulin was infused at 4 mU/kg per min for HFF rats and at 12 mU/kg per min for ZDF rats.

Lipid oxidation assay with primary hepatocytes. Methods were modified from the previous methods (32). Briefly, primary hepatocytes were isolated by the Yale Liver Center from HFF rats treated with control or pyruvate carboxylase ASO for 4 weeks. After recovery, cells were incubated with [1-^{13}C]oleate (GE Healthcare Biosciences, Piscataway, NJ) or [1-^{13}C]palmitate (PerkinElmer, Inc., San Jose, CA) in sealed flasks containing a center well supplied with a clean filter paper. After 1 h, incubations were quenched with 30% perchloric acid and 2 mol/L NaOH to collect [$^{13}CO_2$], which was quantified by scintillation counting. Perchloric acid-soluble ^{13}C-radioactivity (representing ketone bodies, acyl-carnitine, and Krebs cycle intermediates) was also quantified. Counts were normalized to protein content.

In vivo de novo lipogenesis assay (assessment of ^{2}H labeling in triglyceride palmitate). This assay was performed as described previously (26).

In vivo whole-body lipolysis assay. This assay was performed as described previously (26).

Glyceroneogenesis assay. This assay was done as previously described (33). The "% total newly made triglyceride-glycerol" was calculated using the Eq (33): {% total newly made triglyceride-glycerol = [^{2}H-labeling of triglyceride-glycerol/(^{2}H-labeling of plasma × n)] × 100}, where ^{2}H-labeling of triglyceride-glycerol is the M1 isotopomer, the ^{2}H-labeling of plasma is the average labeling in a given rat, and n is the number of exchangeable hydrogens. Previous studies have experimentally measured this value as 4.25 in vivo (34).

Statistical analysis. Linear regression analysis of the data was performed using GraphPad Prism 5.0 software. Data were compared using the Student unpaired t test or ANOVA with the Tukey post hoc test between two groups or more than two groups, respectively. For the lipid oxidation assay, the average of control ASO group was set as 1 every time and the assay was repeated five times and compared using paired t test; each replicate was a separate animal. All data are expressed as mean ± SE, unless otherwise indicated. P values of less than 0.05 were considered significant.

RESULTS

Pyruvate carboxylase protein was increased parallel to glycemic level in humans. We assessed mRNA and protein expression of four gluconeogenic enzymes in human liver biopsy samples obtained from 20 patients undergoing bariatric surgery (Table 1) in relation to measures of glycemia assessed by fasting plasma glucose concentration and hemoglobin A_{1c} (HbA_{1c}). Although none of these patients had a prior diagnosis of type 2 diabetes, there was still a range of fasting plasma glucose concentrations and HbA_{1c}. The protein expression of the other gluconeogenic enzymes (mitochondrial and cytosolic PEPCK, FBP1, and G6PC) did not relate to fasting plasma glucose (data not shown) or HbA_{1c} (Supplementary Fig. 2). Expression of pyruvate carboxylase mRNA expression also did not relate with measures of glycemia (Fig. 1*A* and *B*). In humans, three known isoforms of pyruvate carboxylase mRNA differ in the

TABLE 1
Characteristics of participants

Participants *(N)*	20
Sex (*n*)	
Female	14
Male	6
Age (years)	41.5 ± 2.7
BMI (kg/m^2)	48.4 ± 1.8
Fasting plasma glucose (mg/dL)	99.8 ± 4.0
Fasting plasma insulin (μU/mL)	23.3 ± 2.0
HbA_{1c} (%)	5.8 ± 0.2
HOMA-IR [(mg/dL) × (μU/mL)]	5.4 ± 0.6
Alanine aminotransferase (IU/L)	30.8 ± 3.2
Aspartate aminotransferase (IU/L)	26.6 ± 2.1
LDL cholesterol (mmol/L)	2.84 ± 0.24
HDL cholesterol (mmol/L)	1.09 ± 0.04
Triglyceride (mmol/L)	1.73 ± 0.28

HOMA-IR, homeostatic model assessment of insulin resistance index.

first exon; however, expression of these isoforms also did not correlate with glycemia (Supplementary Fig. 1). In contrast, pyruvate carboxylase protein expression closely related to plasma glucose concentrations, accounting for 52% of the variation in HbA_{1c} (Fig. 1*C* and *D*). Thus, of all the key gluconeogenic enzymes, hepatic pyruvate carboxylase expression best relates to glycemia in humans.

Pyruvate carboxylase ASO treatment was well tolerated and decreased plasma glucose concentrations in regular chow-fed rats. To determine the extent to which pyruvate carboxylase controls endogenous glucose production in vivo, we treated regular chow-fed and HFF male SD rats with pyruvate carboxylase ASO. Pyruvate carboxylase ASO treatment decreased hepatic and adipose pyruvate carboxylase mRNA expressions ~80–90% in regular chow-fed and HFF rats. Hepatic and adipose pyruvate carboxylase protein expressions were decreased ~70–90% (Fig. 2). Pyruvate carboxylase mRNA expression was also slightly decreased in gastrocnemius and kidney cortex, but this did not reduce protein expression in these tissues (Supplementary Fig. 3). Interestingly, HFF per se increased hepatic pyruvate carboxylase protein expression relative to regular chow-fed rats, without changes in mRNA expression, reminiscent of the observation in human liver. In the cohort of rats treated with a control ASO, we found that ubiquitination of pyruvate carboxylase was decreased in livers of HFF rats relative to regular chow-fed rats (Supplementary Fig. 4). This may decrease protein degradation in the ubiquitin-proteasome system and allow for accumulation of pyruvate carboxylase protein out of proportion with changes in mRNA expression.

Pyruvate carboxylase ASO treatment did not have any apparent toxicity; plasma transaminase and lactate concentrations were not different from control ASO-treated chow-fed or HFF rats (Supplementary Table 1). Pyruvate carboxylase ASO decreased fasting and ad lib–fed plasma glucose concentrations in regular chow-fed rats (Fig. 3*A* and *C*). Plasma glucose excursion after a mixed-meal tolerance test was slightly but significantly reduced, without alterations in the plasma insulin secretion (Fig. 3*D* and *F*). To assess the effect of pyruvate carboxylase ASO on glucose production from pyruvate, we performed a pyruvate

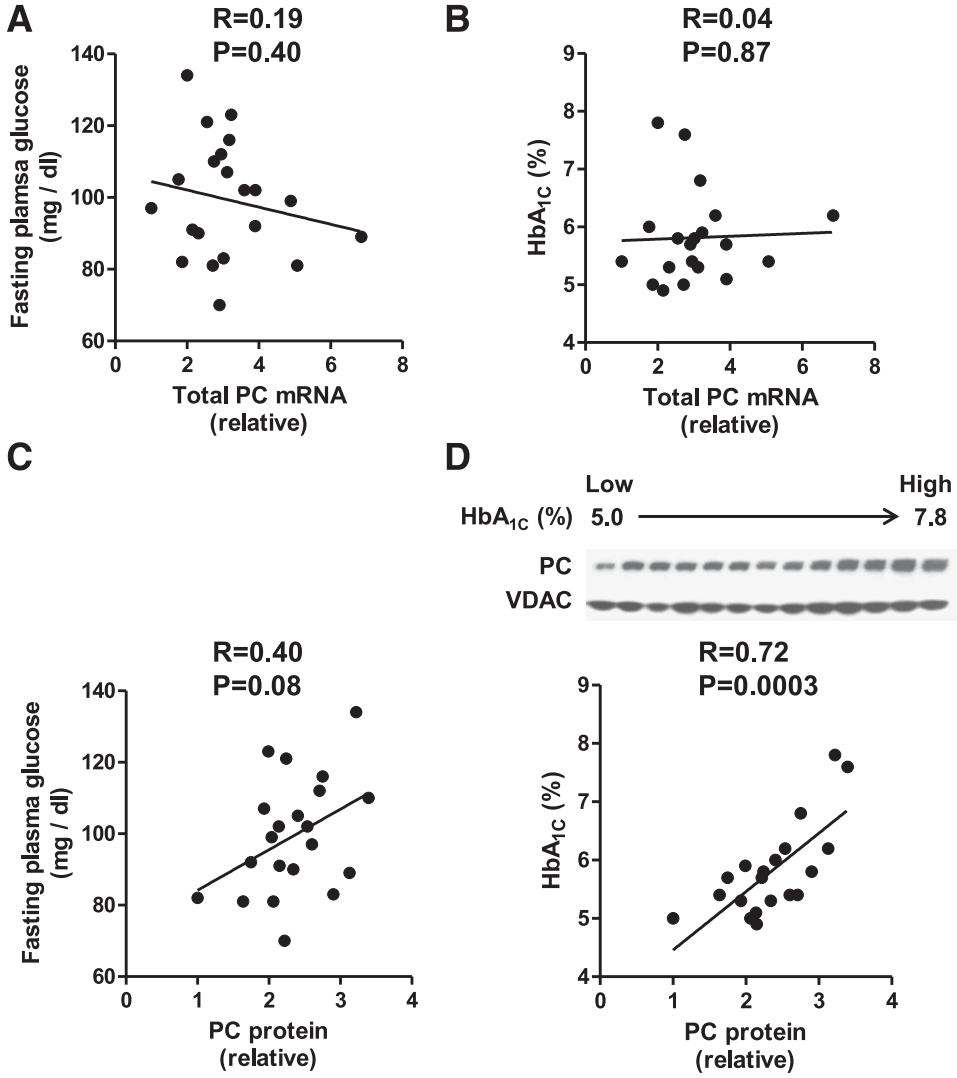

FIG. 1. Hepatic pyruvate carboxylase (PC) protein expression levels relate to glycemic levels in humans. Hepatic PC mRNA expression in human livers compared with fasting plasma glucose concentration (*A*) and HbA_{1c} (*B*). Hepatic PC protein expression in human livers compared with fasting plasma glucose concentration (*C*) and HbA_{1c}, along with representative bands (*D*). PC mRNA and protein are expressed as a relative increase to the lowest expression in the data set (n = 20). VDAC, voltage-dependent anion channel.

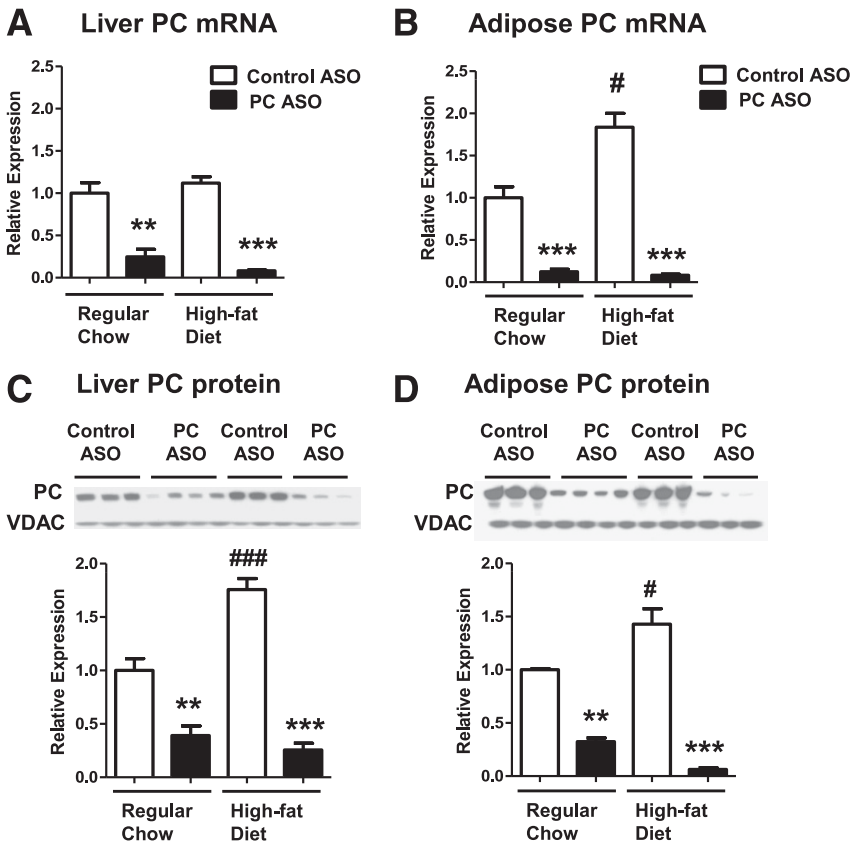

FIG. 2. Pyruvate carboxylase (PC) ASO decreased PC expression in liver and epididymal adipose tissue. PC mRNA in liver (*A*) and epididymal adipose tissue (*B*). PC protein, with representative bands, is shown in liver (*C*) and epididymal adipose tissue (*D*). ***P* < 0.01 and ****P* < 0.001 compared with control ASO group in the same diet condition. #*P* < 0.05 and ###*P* < 0.001 compared with control ASO group in regular chow-fed condition (*n* = 3–4 per group in regular chow-fed condition; *n* = 9–10 per group in HFF condition). All rats were killed and tissues were taken at 4 weeks of treatment. VDAC, voltage-dependent anion channel.

tolerance test in regular chow-fed and HFF rats treated with a control ASO or pyruvate carboxylase ASO. We found that glucose excursion was significantly suppressed by pyruvate carboxylase ASO in the regular chow-fed condition (Fig. 3*G*). The decrease in glucose production was even more marked in HFF rats. Consistent with this observation in vivo, the glucose production from pyruvate in primary hepatocytes isolated from regular chow-fed SD rats was significantly reduced by pyruvate carboxylase suppression by pyruvate carboxylase ASO transfection (Supplementary Fig. 5). Taken together, pyruvate carboxylase ASO treatment reduced hepatic gluconeogenic capacity with a reduction in fasting and fed glucose concentration. This was well tolerated, without evidence for hepatotoxicity, lactic acidosis, or suppression of insulin secretion.

Pyruvate carboxylase ASO reduced adiposity and hepatic steatosis in HFF rats. Interestingly, pyruvate carboxylase ASO also protected HFF rats from weight gain (Fig. 4*A*) and adiposity (Fig. 4*B*). Unlike some lipoatrophic and lipodystrophic models, the reduction in adiposity was associated with a decrease in hepatic triglyceride content (Fig. 4*C*), which was not observed in the regular chow-fed condition (Supplementary Fig. 6). There was no change in skeletal muscle triglyceride content (Fig. 3*D*). Of note, pyruvate carboxylase ASO also reduced plasma fatty acids and cholesterol concentrations in regular chow-fed SD rats and in HFF SD rats (Supplementary Table 1).

To further characterize the mechanism whereby pyruvate carboxylase ASO protected animals from adiposity, we treated HFF male C57BL/6 mice with pyruvate carboxylase ASO and assessed body composition by ^{1}H magnetic resonance spectroscopy and also whole-body energy expenditure and food intake in metabolic cages. As in HFF rats, pyruvate carboxylase ASO decreased body weight gain and fat mass over time. The reduction in weight gain was attributable to a decrease in fat mass; lean body mass was preserved (Supplementary Fig. 7*A* and *B*). Whole-body energy balance was assessed using metabolic cages at 5 weeks of treatment, before any significant difference in body weight, allowing us to assess energy balance without the confounding effects introduced with divergent body weights. Reduction in adiposity and hepatic triglyceride content occurred without any measurable increases in whole-body energy expenditure or reduction in food intake in the mice treated with pyruvate carboxylase ASO (Supplementary Fig. 7*C* and *D*).

Although these measurements were preformed when body weight was matched, we also analyzed the relationship between whole-body energy expenditure and body mass, which was similar between the groups by ANCOVA analysis (i.e., the slopes were not different between the groups [$P = 0.83$]), suggesting that pyruvate carboxylase ASO decreased adiposity without measurable changes in whole-body energy balance. In addition, there was no difference in the respiratory exchange ratio between pyruvate carboxylase and control ASO groups (0.836 ± 0.003 and 0.831 ± 0.005, respectively). Thus, in HFF rodents, decreasing pyruvate carboxylase expression in liver and

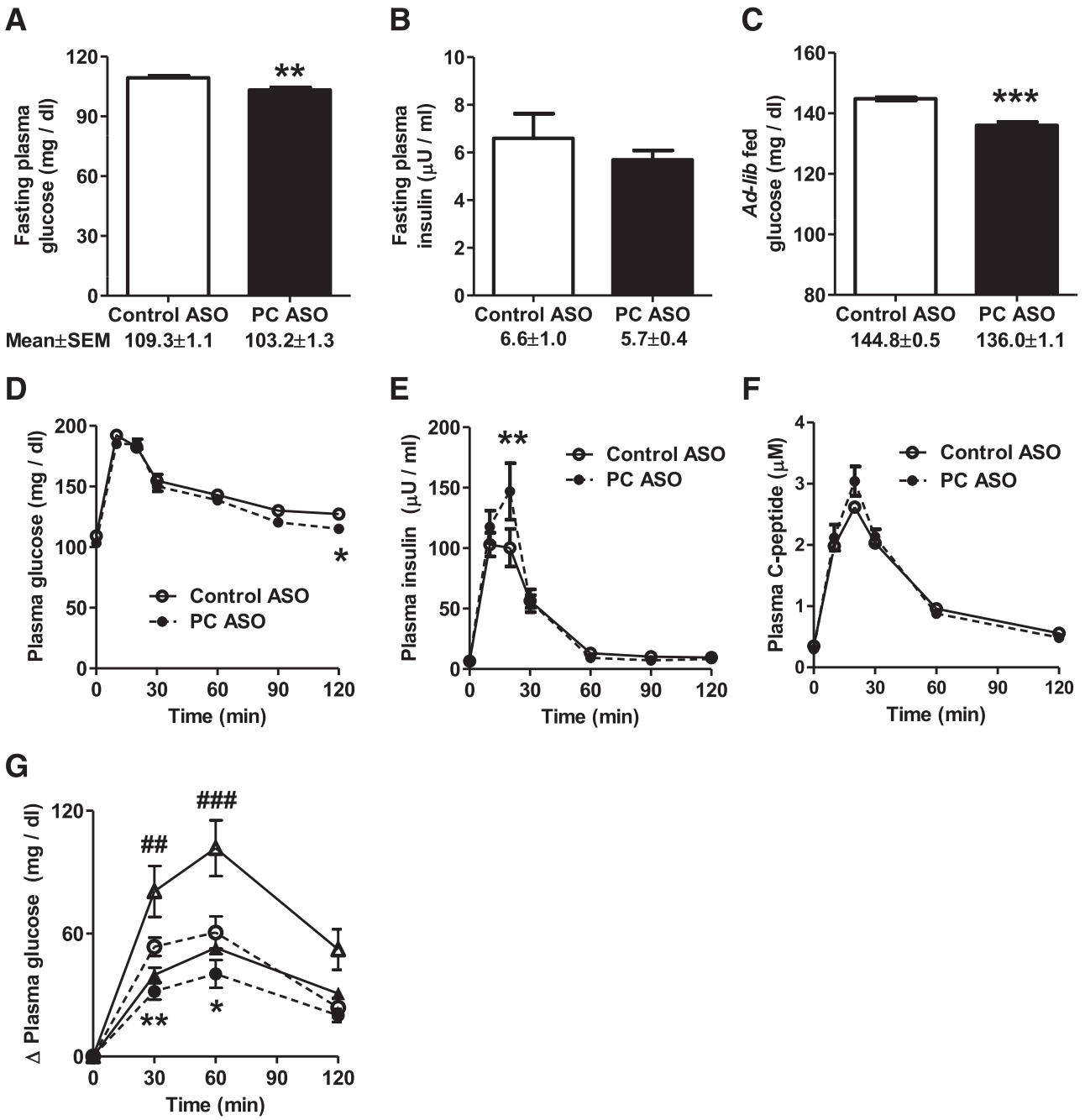

FIG. 3. Pyruvate carboxylase (PC) ASO decreased plasma glucose concentration and did not decrease insulin secretion. Fasting plasma glucose (*A*) and insulin concentration (*B*) in the regular chow-fed rats (n = 7–10 per group). *C*: Ad lib–fed plasma glucose concentration in the regular chow-fed rats (n = 5 per group). Results of mixed-meal tolerance test in the regular chow-fed rats for plasma glucose (*D*), plasma insulin (*E*), and plasma C-peptide (*F*) (n = 7–10). *G*: Pyruvate tolerance test in the regular chow-fed and HFF rats. ○ are control ASO and ● are PC ASO in regular chow-fed rats (both n = 9). △ are control ASO and ▲ are PC ASO in HFF rats (both n = 8). *P < 0.05, **P < 0.01, and ***P < 0.001 between control and PC ASO in regular chow-fed rats; ##P < 0.01 and ###P < 0.001 between control and PC ASO in HFF rats. Experiments were done at 4–5 weeks of treatment.

adipose tissue protects against hepatic steatosis and adiposity without affecting lean body mass or measurable changes in whole-body energy expenditure and food intake.

Pyruvate carboxylase ASO improved hepatic insulin sensitivity in HFF rats. Hepatic steatosis has been associated with insulin resistance, at least partly by diacylglycerol (DAG)-mediated activation of PKCε and impairment of insulin signaling in rodents and humans (27,31,35). We performed hyperinsulinemic-euglycemic clamp studies in HFF rats to assess if pyruvate carboxylase ASO altered insulin sensitivity (Fig. 5). Pyruvate carboxylase ASO reduced fasting plasma glucose concentrations and basal rates of hepatic glucose production without increasing plasma insulin concentration, as expected (Fig. 5*A*–*C*). Insulin-stimulated peripheral glucose metabolism, which largely reflects insulin-stimulated skeletal muscle glucose uptake, was unchanged (Fig. 5*D*-F), without any changes in muscle triglyceride content (Fig. 4*D*). In contrast, pyruvate carboxylase ASO improved hepatic insulin sensitivity as reflected by a ~50% reduction in hepatic glucose production and

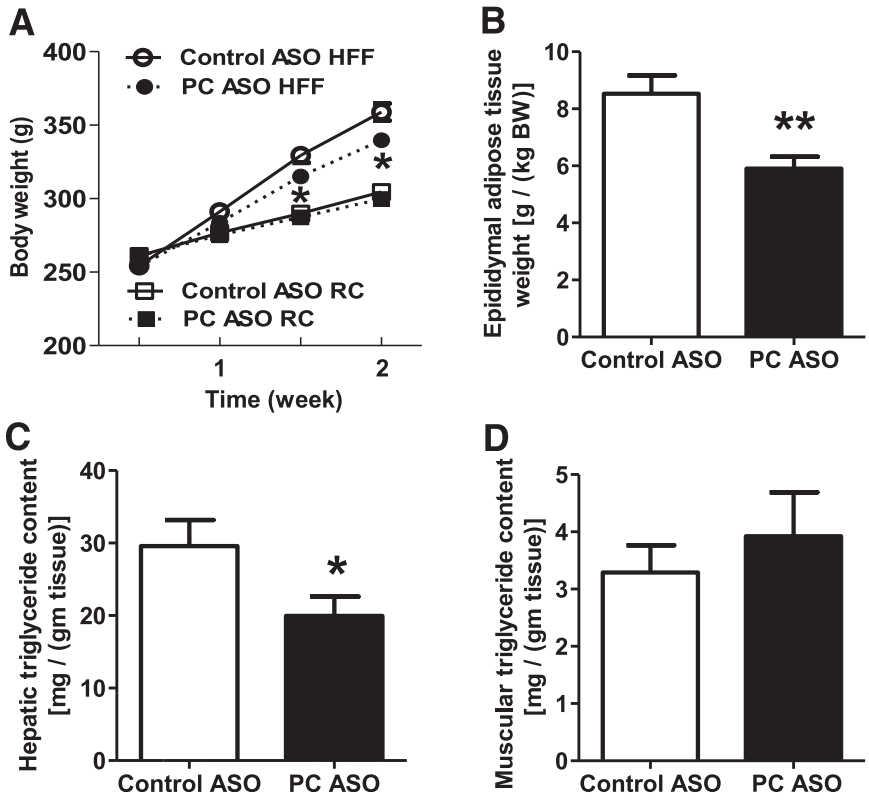

FIG. 4. Pyruvate carboxylase (PC) ASO reduced adiposity and hepatic steatosis in HFF rats. *A*: Body weight (BW) time course in regular chow-fed (n = 10–11 per group) and HFF rats (n = 12 per group). Epididymal adipose tissue weight (*B*), hepatic triglyceride content (*C*), and muscular triglyceride content (*D*) at 4 weeks of treatment in HFF rats (n = 9–10 per group). *$P < 0.05$ and **$P < 0.01$ compared with control ASO group in HFF condition. RC, regular chow.

greater suppression of endogenous glucose production compared with the control ASO–treated rats during the hyperinsulinemic-euglycemic clamp (Fig. 5*G* and *H*). To determine the mechanisms underlying the improvement in hepatic insulin sensitivity, we assessed hepatic DAG content, PKCε activation, and Akt phosphorylation. Pyruvate carboxylase ASO treatment decreased hepatic DAG content in cytosol and membrane fractions, decreased activation of PKCε, and increased insulin-mediated hepatic Akt Ser^{367} phosphorylation (Fig. 6), a key node of the insulin-signaling pathway (35).

Pyruvate carboxylase ASO was also effective in ZDF rats. We also tested the efficacy of pyruvate carboxylase ASO in ZDF rats, a widely used preclinical model of type 2 diabetes. In chow-fed ZDF rats, pyruvate carboxylase ASO lowered the fasting plasma glucose concentration and rates of endogenous glucose production during basal and hyperinsulinemic periods, and suppression of endogenous glucose production by insulin was greater in pyruvate carboxylase ASO–treated rats than in control ASO–treated rats (Supplementary Fig. 8).

Reduction in glyceroneogenesis is the primary mechanism causing reduction in adiposity and hepatic steatosis. To further assess the mechanisms underlying the reduction in adiposity and hepatic steatosis, we performed a series of studies to quantify whole body lipolysis, lipid oxidation, de novo fatty acid synthesis, and glycerol synthesis in HFF rats (Supplementary Fig. 9). Pyruvate carboxylase is involved in adipogenesis (36–39); however, the adipose expressions of key genes associated with adipogenesis, such as peroxisome proliferator activated receptor (PPAR) γ, adiponectin, cluster of differentiation (CD) 36, and adipocyte protein (aP) 2, were not altered by pyruvate carboxylase ASO (Supplementary Table 2). Pyruvate carboxylase ASO did slightly decrease adipose mRNA expression of adipocyte triglyceride lipase (ATGL) and patatin-like phospholipase domain-containing 3 (PNPLA3) (Supplementary Table 2), and also decreased plasma nonesterified fatty acid concentration (Supplementary Table 1). However, no difference occurred in the rates of whole-body lipolysis as assessed by glycerol turnover (Fig. 7*A*). There was no difference in the rates of fatty acid oxidation measured using primary hepatocytes isolated from control ASO or pyruvate carboxylase ASO–treated rats (Fig. 7*B* and *C*) or in the expression of genes regulating fatty acid oxidation in liver and adipose tissue (Supplementary Table 2).

We quantified hepatic de novo lipogenesis by measuring ^2H_2O incorporation into triglyceride palmitate in vivo. Neither the percentage of de novo fatty acid synthesis (Fig. 7*D*) nor the expression of lipogenic genes in liver (Supplementary Table 2) was altered. Adipose sterol regulatory element binding transcription factor 1c (SREBP1c) mRNA expression was decreased by pyruvate carboxylase ASO treatment, but the downstream genes, such as acetyl-CoA carboxylase 1 (ACC1) and fatty acid synthase (FAS), were not decreased (Supplementary Table 2). However, pyruvate carboxylase ASO decreased glycerol synthesis in liver and adipose tissue, as measured by the incorporation of ^2H_2O into triglyceride-glycerol (i.e., the glycerol backbone of a triglyceride molecule, Fig. 7*E* and *F*). This method quantifies total new glycerol synthesis, which includes glyceroneogenesis and formation of glycerol from glucose. In HFF conditions, however, glyceroneogenesis is thought important for the production of glycerol 3-phosphate (33)

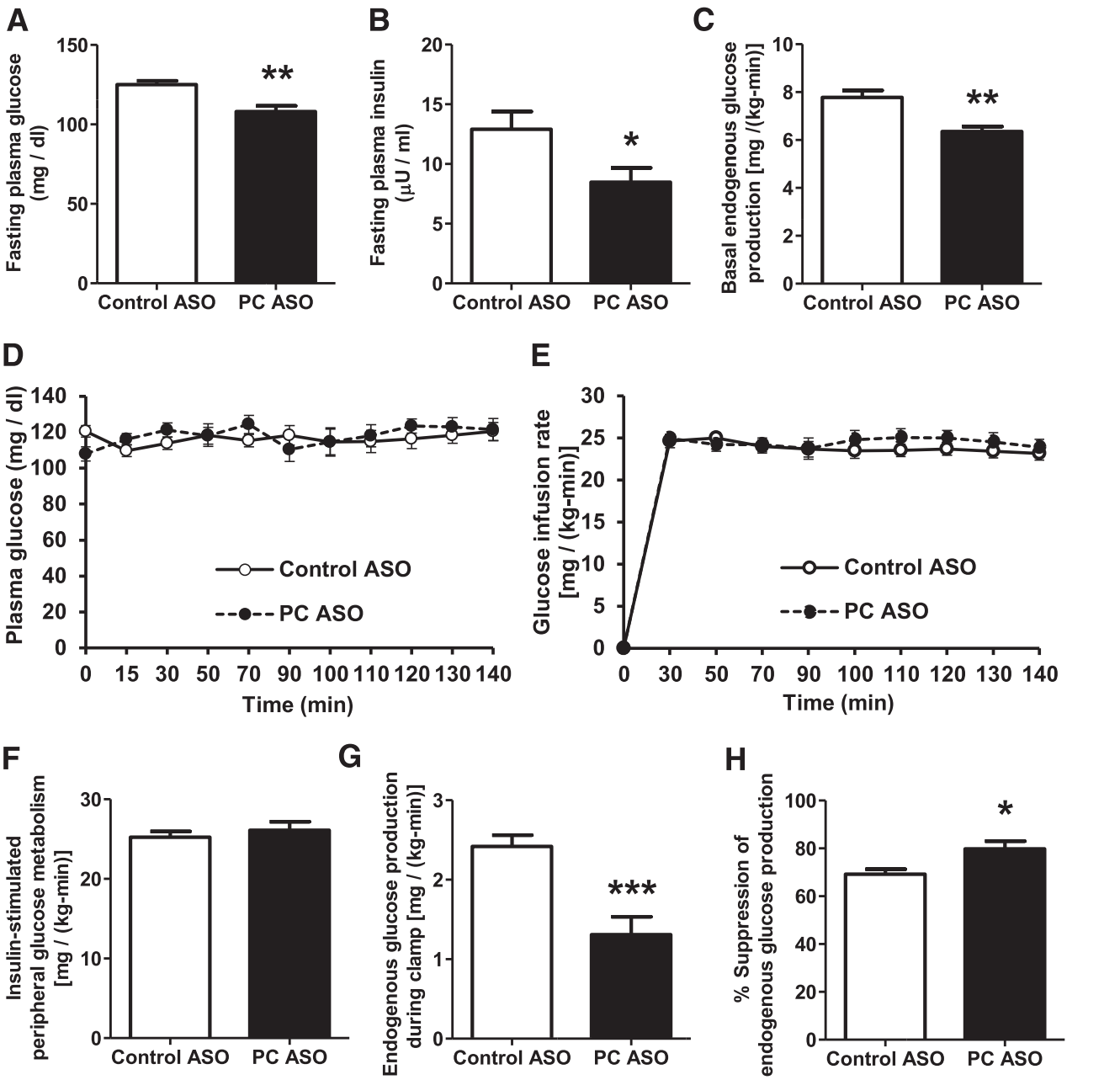

FIG. 5. Pyruvate carboxylase (PC) ASO improves hepatic insulin sensitivity in HFF rats. Fasting plasma glucose (*A*) and insulin concentration (*B*) (n = 9 per group). *C*: Basal endogenous glucose production (n = 9 per group). Plasma glucose concentration (*D*) and glucose infusion rate time course (*E*) during hyperinsulinemic-euglycemic (4 mU/kg per min) clamp, respectively (n = 7–8 per group). Insulin-stimulated peripheral glucose metabolism (*F*), endogenous glucose production (*G*), and percentage suppression of endogenous glucose production (*H*) during clamp (n = 7–8 per group). *P < 0.05, **P < 0.01, and ***P < 0.001 compared with control ASO group. Experiments were done at 4–5 weeks of treatment.

for the esterification and storage of fatty acids as triglyceride (Supplementary Fig. 9). Therefore, reduced glyceroneogenesis may be the primary mechanism accounting for the reduction in adiposity and hepatic steatosis in HFF rodents (Fig. 7*G*).

DISCUSSION

Patients with type 2 diabetes have increased gluconeogenesis (1,3,40,41). The molecular links between islet hormones and transcription of PEPCK and G6PC supported a view that increased gluconeogenesis was a consequence of increased transcription of these enzymes (9–12). However, we previously reported that the expression of PEPCK and G6PC mRNA did not relate to fasting hyperglycemia in rodent models of type 2 diabetes or in humans with type 2 diabetes (17). We now extend this initial observation, demonstrating that increases in pyruvate carboxylase protein expression, but not mRNA expression, better relate to glycemia than expression of the other gluconeogenic enzymes. Using an ASO approach to reduce pyruvate carboxylase protein expression, we quantified the changes in glucose and lipid metabolism in vivo. We demonstrated that decreasing pyruvate carboxylase expression in liver and adipose tissue is well tolerated and effective in decreasing basal rates of endogenous glucose production and plasma glucose

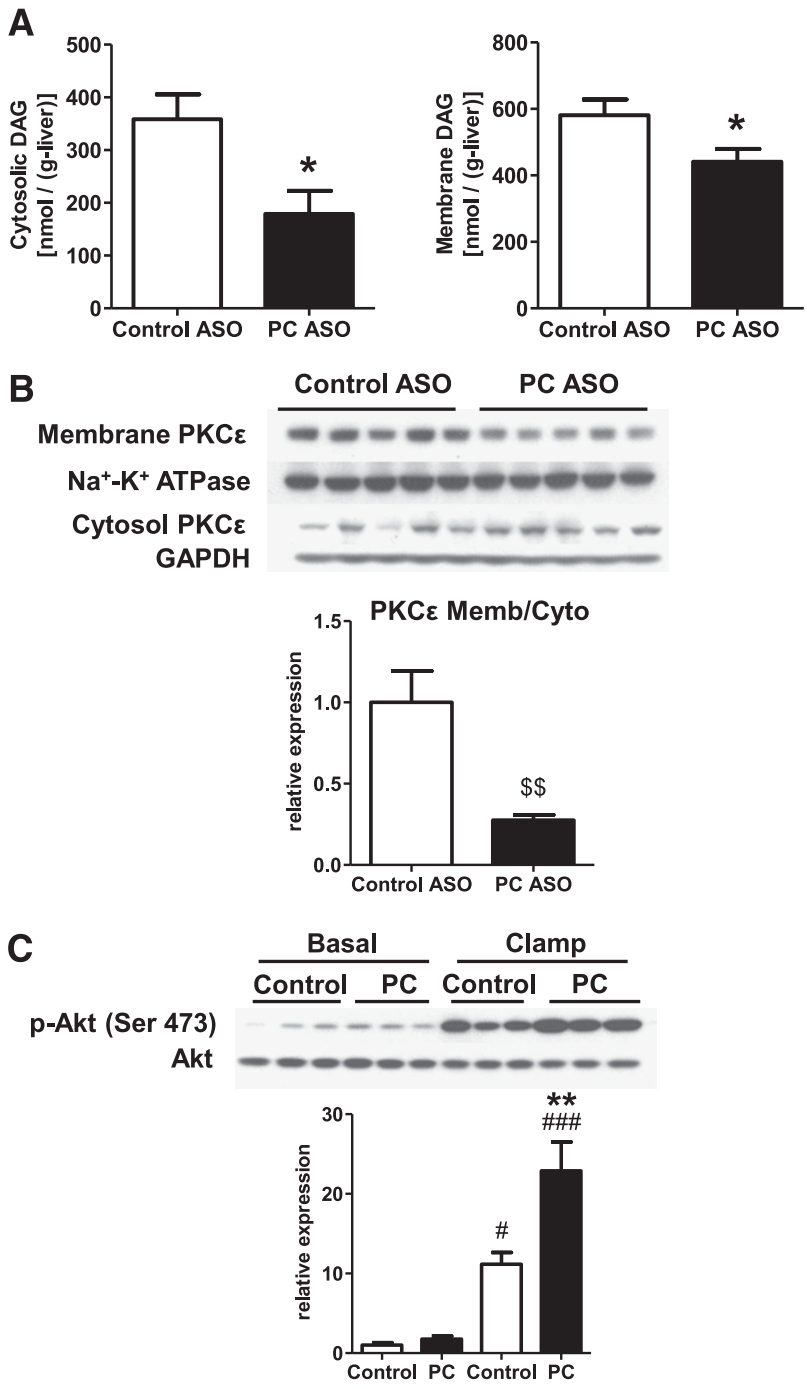

FIG. 6. Pyruvate carboxylase (PC) ASO decreased hepatic DAG content and PKCε activation and increased hepatic Akt phosphorylation in HFF rats. *A*: Hepatic DAG content (n = 9–10 per group). *P < 0.05 compared with control ASO group. *B*: PKCε activation. The average of control ASO group was set as 1 (n = 5 per group). GAPDH, glyceraldehyde-3-phosphate dehydrogenase. \$\$$P$ < 0.001 compared with control ASO group. *C*: Akt phosphorylation (Ser^{473}). The average expression of control ASO group in the basal condition was set as 1 (n = 5 per group). #P < 0.05 and ###P < 0.001 compared with control ASO group in basal condition. **P < 0.01 compared with control ASO group in clamp condition. All tissues were taken at 4–5 weeks of treatment.

concentrations. In addition, we observed a reduction of adiposity and hepatic steatosis in HFF rats, with improvements in hepatic insulin sensitivity in HFF rats and ZDF rats. The changes in lipid metabolism are likely a consequence of decreased glycerol synthesis in liver and adipose tissue and highlight the importance of pyruvate carboxylase in supporting glyceroneogenesis in vivo.

We first quantified the expression of the key rate-controlling gluconeogenic enzymes in liver biopsy specimens obtained from human subjects undergoing elective surgery and related the expression of these enzymes to plasma glucose concentration and HbA_{1c}. Only pyruvate carboxylase protein expression correlated to glycemia in this cohort. The relationship between pyruvate carboxylase protein and HbA_{1c} was stronger than the relationship with fasting plasma glucose concentrations, raising the possibility that hepatic pyruvate carboxylase expression impacts both fasting and postprandial glucose concentrations. Thus, HbA_{1c}

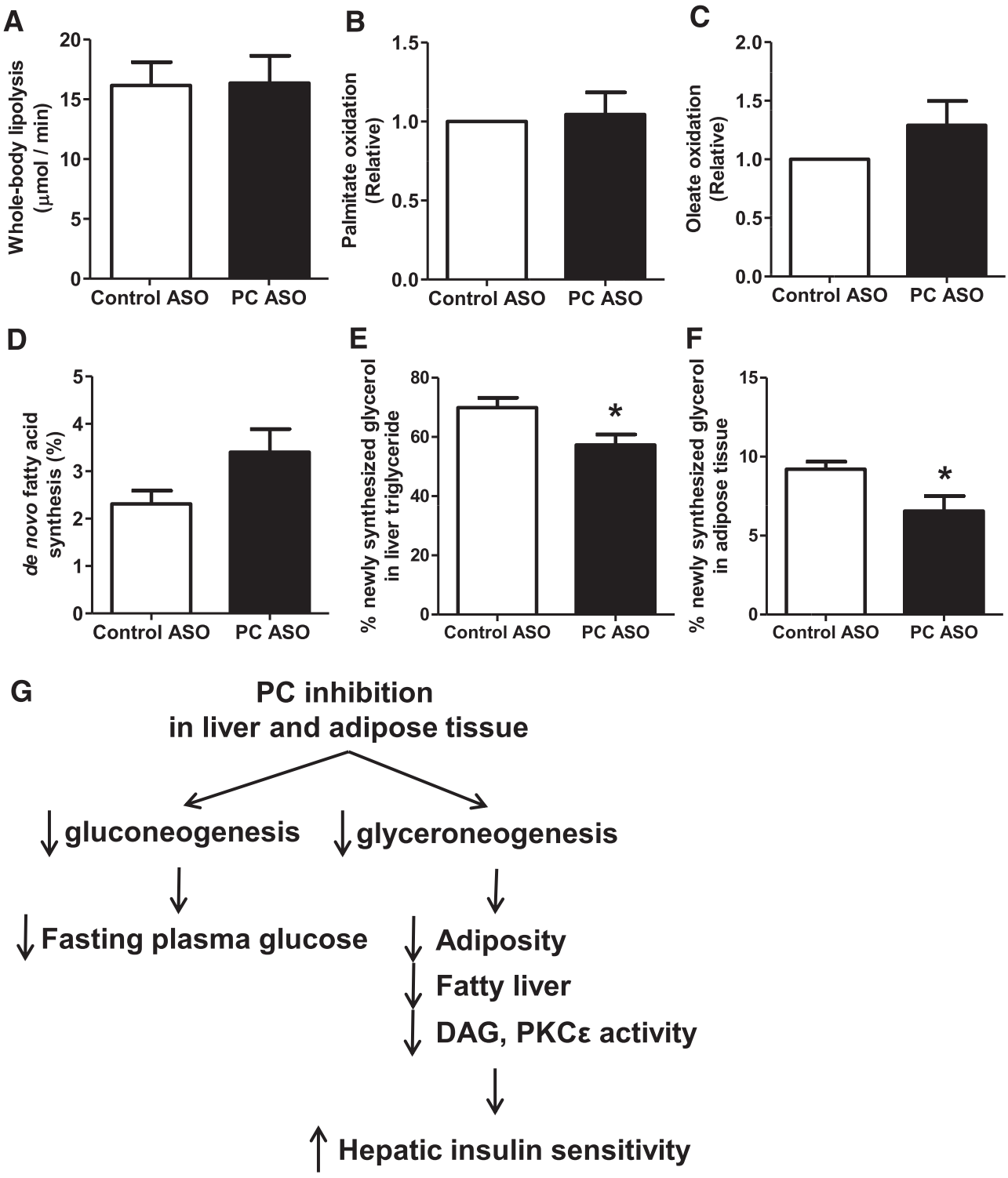

FIG. 7. Pyruvate carboxylase (PC) ASO reduced hepatic and adipose glycerol synthesis. *A*: Whole-body lipolysis as assessed by glycerol turnover in HFF rats (n = 8–9 per group). Palmitate oxidation (*B*) and oleate oxidation (*C*) assay with primary hepatocytes isolated from HFF-treated and ASO-treated rats (n = 5 per group). *D*: In vivo hepatic de novo fatty acid synthesis in HFF rats (n = 9–10 per group). Hepatic (*E*) and adipose glycerol synthesis (*F*) in HFF rats (n = 7–8 per group). *G*: Summary of this study. *$P < 0.05$ compared with control ASO group. All experiments were done at 4–5 weeks of treatment.

better relates to pyruvate carboxylase expression than fasting plasma glucose concentrations. However, it is also possible that a single fasting plasma glucose concentration does not accurately reflect long-term trends of fasting glycemia.

The increase in pyruvate carboxylase protein expression occurred without changes in mRNA, suggesting that other mechanisms affect protein abundance (e.g., post-transcriptional modification). We observed a similar disassociation between pyruvate carboxylase protein and mRNA abundance in HFF rodents compared with chow-fed rodents. We used this model to explore possible mechanisms accounting for the disassociation between pyruvate

carboxylase mRNA and protein expression. Pyruvate carboxylase ubiquitination is decreased in HFF rat liver relative to chow-fed rat liver. This suggests that pyruvate carboxylase degradation in the ubiquitin-proteasome system is decreased, which may result in increased pyruvate carboxylase protein accumulation. This also may provide a possible mechanism that accounts for the increased hepatic pyruvate carboxylase flux that was recently reported in humans with nonalcoholic fatty liver disease (42).

To quantify the role of pyruvate carboxylase in controlling glucose and lipid metabolism, we used a loss-of-function approach. Although phenylalkanoic compounds can acutely reduce hepatic glucose production and plasma glucose concentration (22), these compounds lack tissue specificity and can potentially impair glucose-stimulated insulin secretion (43). Moreover, there are no reports of chronic inhibition of pyruvate carboxylase. ASOs have inherent tissue specificity, effectively silencing gene expression in liver and white adipose tissue but negligibly in muscle, brown adipose tissue, pancreas, brain, or stomach (23,24). This tissue specificity mirrors the two promoters that control pyruvate carboxylase expression (44). The proximal promoter element (P1) is primarily active in liver, adipose, kidney, and the mammary glands. In contrast, the distal promoter element (P2) maintains pyruvate carboxylase expression in many other tissues, including skeletal muscle, β-cells, and astrocytes. These discrete promoters may allow specific tissues to use pyruvate carboxylase as a common means to different ends: for glucose and lipid metabolism in P1-predominant tissues and anaplerosis in P2-predominant tissues. Thus, this approach permits us to assess the effects of decreasing pyruvate carboxylase expression in P1-selective tissues and also serves to vet tissue-targeted inhibition of pyruvate carboxylase expression and activity as a potential treatment for type 2 diabetes.

Decreasing pyruvate carboxylase expression decreased fasting plasma glucose concentrations in regular chow-fed SD rats, HFF SD rats, and ZDF rats. This was associated with a decrease in basal rates of hepatic glucose production in HFF SD rats and ZDF rats. Patients with pyruvate carboxylase deficiency can develop severe lactic acidosis at an early age (45). In contrast, the tissue-specific decrease in pyruvate carboxylase expression by ASO treatment did not result in any hepatotoxicity or lactic acidosis, although there was a small increase in plasma lactate concentrations in ZDF rats. Although ASOs do not decrease β-cell gene expression, we confirmed that insulin secretion was unaffected in mixed-meal tolerance tests in SD rats. Thus, tissue-specific inhibition of pyruvate carboxylase by ASO treatment effectively and safely lowers hepatic glucose production in multiple rodent models in chronic treatment.

Interestingly, pyruvate carboxylase inhibition also profoundly altered lipid metabolism. Pyruvate carboxylase ASO reduced adiposity and hepatic steatosis in HFF rodents. By comparison, liver-specific deletion of PEPCK and inhibition of G6PC resulted in hepatic steatosis (46,47), and inhibition of FBP1 resulted in hyperlipidemia (48). Adipose pyruvate carboxylase expression is reported to be induced during adipogenesis and increased by PPARγ agonists, but there are no data on how inhibition of pyruvate carboxylase may alter lipid metabolism (36–39). Metabolic cage studies in mice treated with pyruvate carboxylase ASO did not reveal increases in whole-body energy expenditure or a reduction in food intake, although it may be possible that changes specific to liver or adipose tissue are not reflected in measures of whole-body energy metabolism.

To better characterize the lipid phenotype, we performed a comprehensive set of studies assessing various components of lipid metabolism. There were no differences in lipolysis, fatty acid oxidation, or de novo fatty acid synthesis. However, we demonstrated that pyruvate carboxylase ASO treatment reduced adipose and hepatic glycerol synthesis in vivo, likely due to a decrease in glyceroneogenesis. Glyceroneogenesis plays a minor role in animals fed high-carbohydrate diets (i.e., low-fat), but its contribution to total glycerol 3-phosphate synthesis increases under fat-fed conditions, accounting for ~50–90% of glycerol 3-phosphate synthesis (33,49,50). This is consistent with our observation that the reduction in adiposity is primarily apparent in fat-fed rodents. Thus, when dietary lipid is in excess, the reduction in adipose and hepatic glycerol synthesis with pyruvate carboxylase ASO may impair lipid esterification and, consequently, lipid storage. In comparison, PEPCK is important for adipose glyceroneogenesis (51) but does not appear to be as essential for hepatic glyceroneogenesis because mice lacking PEPCK can still develop hepatic steatosis (46). By comparison, decreasing pyruvate carboxylase expression by ASO treatment protected mice and rats from adiposity and hepatic steatosis. The subsequent improvement in hepatic insulin sensitivity could be attributed to decreased DAG content and PKCε activation as well as improved insulin-stimulated Akt phosphorylation (31,35,52).

In conclusion, these are the first studies to demonstrate that increased hepatic pyruvate carboxylase protein expression is specifically and closely associated with plasma glycemia in humans, suggesting that hepatic pyruvate carboxylase is a key determinant of hepatic gluconeogenesis in humans. Pyruvate carboxylase ASO decreased liver and adipose expression of this enzyme and lowered plasma glucose concentrations and hepatic glucose production in vivo, without any apparent adverse toxicity. In addition, pyruvate carboxylase ASO decreased adiposity and hepatic steatosis in fat-fed rodents by decreasing adipose and hepatic glycerol synthesis. This, in turn, improved hepatic insulin signaling and hepatic insulin responsiveness. These studies suggest that pyruvate carboxylase is a key regulator of both gluconeogenesis and glyceroneogenesis. Through the latter, pyruvate carboxylase may also regulate lipid metabolism. Taken together these data demonstrate that tissue-specific inhibition of pyruvate carboxylase may be a potential strategy for treating many aspects of the metabolic syndrome and type 2 diabetes.

ACKNOWLEDGMENTS

This project was supported by grants from the United States Public Health Service (R24-DK-085638, R01-DK-40936, R01-AG-23686, R01-DK-088231, R01-DK-34989, UL1-RR-0241395, P30-DK-034989, P30-DK-45735), Manpei Suzuki Diabetes Foundation Fellowship (N.K.), a Distinguished Clinical Scientist Award (K.F.P.) and a Mentor-Based Postdoctoral Fellowship Grant (G.I.S.) from the American Diabetes Association, and a VA Merit Grant (5I01BX000901) (V.T.S.).

V.P.M. and S.B. are employees of ISIS and may own stock in the company. No other potential conflicts of interest relevant to this article were reported.

N.K., S.A.B., D.F.V., S.K.M., J.L.C., F.G.-E., I.F., B.G., M.J.J., A.L.B., M.K., B.K.P., M.A.P., K.F.P., G.W.C., G.I.S., and V.T.S. researched data and were involved in the analysis and

interpretation of data. V.P.M. and S.B. designed, screened, and generated ASOs. C.D.S. and G.S.G. obtained liver biopsy specimens from humans. N.K., G.I.S., and V.T.S. wrote the manuscript. V.T.S. is the guarantor of this work and, as such, had full access to all the data in the study and takes responsibility for the integrity of the data and the accuracy of the data analysis.

Preliminary data from this study were presented at the 70th Scientific Sessions of the American Diabetes Association, Orlando, Florida, 25–29 June 2010, and at the 71st Scientific Sessions of the American Diabetes Association, San Diego, California, 24–28 June 2011.

The authors thank the volunteers for participating in this study, Daryl Granner (Vanderbilt University Medical Center) for his kind gift of C-PEPCK antibody, and Yanna Kosover, Jianying Dong, Kathy Harry, Dongyan Zhang, Toru Yoshimura, Shoichi Kanda, Derek M. Erion, Rebecca L. Pongratz, Codruta Todeasa, Maria Batsu, and Aida Groszmann (all of the Yale University School of Medicine) for their excellent technical support.

REFERENCES

1. Magnusson I, Rothman DL, Katz LD, Shulman RG, Shulman GI. Increased rate of gluconeogenesis in type II diabetes mellitus. A ^{17}C nuclear magnetic resonance study. J Clin Invest 1992;90:1323–1327
2. Maggs DG, Buchanan TA, Burant CF, et al. Metabolic effects of troglitazone monotherapy in type 2 diabetes mellitus. A randomized, double-blind, placebo-controlled trial. Ann Intern Med 1998;128:176–185
3. Hundal RS, Krssak M, Dufour S, et al. Mechanism by which metformin reduces glucose production in type 2 diabetes. Diabetes 2000;49:2063–2069
4. Utter MF, Keech DB. Formation of oxaloacetate from pyruvate and carbon dioxide. J Biol Chem 1960;235:PC17–PC18
5. Weber G, Cantero A. Glucose-6-phosphatase studies in fasting. Science 1954;120:851–852
6. Utter MF, Kurahashi K. Purification of oxalacetic carboxylase from chicken liver. J Biol Chem 1954;207:787–802
7. McGilvery RW, Mokrasch LC. Purification and properties of fructose-1, 6-diphosphatase. J Biol Chem 1956;221:909–917
8. Jurado LA, Song S, Roesler WJ, Park EA. Conserved amino acids within CCAAT enhancer-binding proteins (C/EBP(alpha) and beta) regulate phosphoenolpyruvate carboxykinase (PEPCK) gene expression. J Biol Chem 2002;277:27606–27612
9. Koo SH, Flechner L, Qi L, et al. The CREB coactivator TORC2 is a key regulator of fasting glucose metabolism. Nature 2005;437:1109–1111
10. Nakae J, Kitamura T, Silver DL, Accili D. The forkhead transcription factor Foxo1 (Fkhr) confers insulin sensitivity onto glucose-6-phosphatase expression. J Clin Invest 2001;108:1359–1367
11. O'Brien RM, Noisin EL, Suwanichkul A, et al. Hepatic nuclear factor 3- and hormone-regulated expression of the phosphoenolpyruvate carboxykinase and insulin-like growth factor-binding protein 1 genes. Mol Cell Biol 1995; 15:1747–1758
12. Yoon JC, Puigserver P, Chen G, et al. Control of hepatic gluconeogenesis through the transcriptional coactivator PGC-1. Nature 2001;413:131–138
13. Burgess SC, He T, Yan Z, et al. Cytosolic phosphoenolpyruvate carboxykinase does not solely control the rate of hepatic gluconeogenesis in the intact mouse liver. Cell Metab 2007;5:313–320
14. Le Lay J, Tuteja G, White P, Dhir R, Ahima R, Kaestner KH. CRTC2 (TORC2) contributes to the transcriptional response to fasting in the liver but is not required for the maintenance of glucose homeostasis. Cell Metab 2009;10:55–62
15. Ramnanan CJ, Edgerton DS, Rivera N, et al. Molecular characterization of insulin-mediated suppression of hepatic glucose production in vivo. Diabetes 2010;59:1302–1311
16. Sloop KW, Showalter AD, Cox AL, et al. Specific reduction of hepatic glucose 6-phosphate transporter-1 ameliorates diabetes while avoiding complications of glycogen storage disease. J Biol Chem 2007;282:19113–19121
17. Samuel VT, Beddow SA, Iwasaki T, et al. Fasting hyperglycemia is not associated with increased expression of PEPCK or G6Pc in patients with type 2 diabetes. Proc Natl Acad Sci U S A 2009;106:12121–12126
18. Jitrapakdee S, St Maurice M, Rayment I, Cleland WW, Wallace JC, Attwood PV. Structure, mechanism and regulation of pyruvate carboxylase. Biochem J 2008;413:369–387
19. Weinberg MB, Utter MF. Effect of streptozotocin-induced diabetes mellitus on the turnover of rat liver pyruvate carboxylase and pyruvate dehydrogenase. Biochem J 1980;188:601–608
20. Large V, Beylot M. Modifications of citric acid cycle activity and gluconeogenesis in streptozotocin-induced diabetes and effects of metformin. Diabetes 1999;48:1251–1257
21. Jitrapakdee S, Gong Q, MacDonald MJ, Wallace JC. Regulation of rat pyruvate carboxylase gene expression by alternate promoters during development, in genetically obese rats and in insulin-secreting cells. Multiple transcripts with 5′-end heterogeneity modulate translation. J Biol Chem 1998;273:34422–34428
22. Bahl JJ, Matsuda M, DeFronzo RA, Bressler R. In vitro and in vivo suppression of gluconeogenesis by inhibition of pyruvate carboxylase. Biochem Pharmacol 1997;53:67–74
23. Nagai Y, Yonemitsu S, Erion DM, et al. The role of peroxisome proliferator-activated receptor gamma coactivator-1 beta in the pathogenesis of fructose-induced insulin resistance. Cell Metab 2009;9:252–264
24. Sazani P, Gemignani F, Kang SH, et al. Systemically delivered antisense oligomers upregulate gene expression in mouse tissues. Nat Biotechnol 2002;20:1228–1233
25. Chu X, Erdman R, Susek M, et al. Association of morbid obesity with FTO and INSIG2 allelic variants. Arch Surg 2008;143:235–240; discussion 241
26. Kumashiro N, Yoshimura T, Cantley JL, et al. Role of patatin-like phospholipase domain-containing 3 on lipid-induced hepatic steatosis and insulin resistance in rats. Hepatology 2013;57:1763–1772
27. Kumashiro N, Erion DM, Zhang D, et al. Cellular mechanism of insulin resistance in nonalcoholic fatty liver disease. Proc Natl Acad Sci U S A 2011;108:16381–16385
28. Wiese TJ, Lambeth DO, Ray PD. The intracellular distribution and activities of phosphoenolpyruvate carboxykinase isozymes in various tissues of several mammals and birds. Comp Biochem Physiol B 1991;100:297–302
29. Petrescu I, Bojan O, Saied M, Bârzu O, Schmidt F, Kühnle HF. Determination of phosphoenolpyruvate carboxykinase activity with deoxyguanosine 5′-diphosphate as nucleotide substrate. Anal Biochem 1979;96: 279–281
30. Kumashiro N, Tamura Y, Uchida T, et al. Impact of oxidative stress and peroxisome proliferator-activated receptor gamma coactivator-1alpha in hepatic insulin resistance. Diabetes 2008;57:2083–2091
31. Samuel VT, Liu ZX, Wang A, et al. Inhibition of protein kinase Cepsilon prevents hepatic insulin resistance in nonalcoholic fatty liver disease. J Clin Invest 2007;117:739–745
32. Birkenfeld AL, Lee HY, Guebre-Egziabher F, et al. Deletion of the mammalian INDY homolog mimics aspects of dietary restriction and protects against adiposity and insulin resistance in mice. Cell Metab 2011;14:184–195
33. Bederman IR, Foy S, Chandramouli V, Alexander JC, Previs SF. Triglyceride synthesis in epididymal adipose tissue: contribution of glucose and non-glucose carbon sources. J Biol Chem 2009;284:6101–6108
34. Turner SM, Murphy EJ, Neese RA, et al. Measurement of TG synthesis and turnover in vivo by 2H2O incorporation into the glycerol moiety and application of MIDA. Am J Physiol Endocrinol Metab 2003;285:E790–E803
35. Samuel VT, Shulman GI. Mechanisms for insulin resistance: common threads and missing links. Cell 2012;148:852–871
36. Jitrapakdee S, Vidal-Puig A, Wallace JC. Anaplerotic roles of pyruvate carboxylase in mammalian tissues. Cell Mol Life Sci 2006;63:843–854
37. Jitrapakdee S, Slawik M, Medina-Gomez G, et al. The peroxisome proliferator-activated receptor-gamma regulates murine pyruvate carboxylase gene expression in vivo and in vitro. J Biol Chem 2005;280:27466–27476
38. Wellen KE, Uysal KT, Wiesbrock S, Yang Q, Chen H, Hotamisligil GS. Interaction of tumor necrosis factor-alpha- and thiazolidinedione-regulated pathways in obesity. Endocrinology 2004;145:2214–2220
39. Wilson-Fritch L, Nicoloro S, Chouinard M, et al. Mitochondrial remodeling in adipose tissue associated with obesity and treatment with rosiglitazone. J Clin Invest 2004;114:1281–1289
40. Cobelli C, Mari A, Duner E, Mollo F, Nosadini R. On the estimation of absorption of subcutaneous injected insulin from plasma concentrations using mathematical models. Diabetologia 1984;26:314–316
41. Woerle HJ, Szoke E, Meyer C, et al. Mechanisms for abnormal postprandial glucose metabolism in type 2 diabetes. Am J Physiol Endocrinol Metab 2006;290:E67–E77
42. Sunny NE, Parks EJ, Browning JD, Burgess SC. Excessive hepatic mitochondrial TCA cycle and gluconeogenesis in humans with nonalcoholic fatty liver disease. Cell Metab 2011;14:804–810
43. Farfari S, Schulz V, Corkey B, Prentki M. Glucose-regulated anaplerosis and cataplerosis in pancreatic beta-cells: possible implication of a pyruvate/citrate shuttle in insulin secretion. Diabetes 2000;49:718–726

44. Jitrapakdee S, Booker GW, Cassady AI, Wallace JC. The rat pyruvate carboxylase gene structure. Alternate promoters generate multiple transcripts with the 5′-end heterogeneity. J Biol Chem 1997;272:20522–20530
45. Marin-Valencia I, Roe CR, Pascual JM. Pyruvate carboxylase deficiency: mechanisms, mimics and anaplerosis. Mol Genet Metab 2010;101:9–17
46. Burgess SC, Hausler N, Merritt M, et al. Impaired tricarboxylic acid cycle activity in mouse livers lacking cytosolic phosphoenolpyruvate carboxykinase. J Biol Chem 2004;279:48941–48949
47. Bandsma RH, Wiegman CH, Herling AW, et al. Acute inhibition of glucose-6-phosphate translocator activity leads to increased de novo lipogenesis and development of hepatic steatosis without affecting VLDL production in rats. Diabetes 2001;50:2591–2597
48. van Poelje PD, Potter SC, Chandramouli VC, Landau BR, Dang Q, Erion MD. Inhibition of fructose 1,6-bisphosphatase reduces excessive endogenous glucose production and attenuates hyperglycemia in Zucker diabetic fatty rats. Diabetes 2006;55:1747–1754
49. Chen JL, Peacock E, Samady W, et al. Physiologic and pharmacologic factors influencing glyceroneogenic contribution to triacylglyceride glycerol measured by mass isotopomer distribution analysis. J Biol Chem 2005;280:25396–25402
50. Nye CK, Hanson RW, Kalhan SC. Glyceroneogenesis is the dominant pathway for triglyceride glycerol synthesis in vivo in the rat. J Biol Chem 2008;283:27565–27574
51. Millward CA, Desantis D, Hsieh CW, et al. Phosphoenolpyruvate carboxykinase (Pck1) helps regulate the triglyceride/fatty acid cycle and development of insulin resistance in mice. J Lipid Res 2010;51:1452–1463
52. Samuel VT, Liu ZX, Qu X, et al. Mechanism of hepatic insulin resistance in non-alcoholic fatty liver disease. J Biol Chem 2004;279:32345–32353